

^1H NMR and Molecular Dynamics Evidence for an Unexpected Interaction on the Origin of Salting-In/Salting-Out Phenomena

Mara G. Freire,[†] Catarina M. S. S. Neves,[‡] Artur M. S. Silva,[§] Luís M. N. B. F. Santos,^{||} Isabel M. Marrucho,^{†,‡} Luís P. N. Rebelo,[†] Jindal K. Shah,[⊥] Edward J. Maginn,[⊥] and João A. P. Coutinho^{*,‡}

Instituto de Tecnologia Química e Biológica, ITQB2, Universidade Nova de Lisboa, Av. República, Apartado 127, 2780-901 Oeiras, Portugal, CICECO, Departamento de Química, Universidade de Aveiro, 3810-193 Aveiro, Portugal, QOPNA, Departamento de Química, Universidade de Aveiro, 3810-193 Aveiro, Portugal, CIQ, Departamento de Química, Faculdade de Ciências da Universidade do Porto, R. Campo Alegre 687, 4169-007 Porto, Portugal, and Department of Chemical and Biomolecular Engineering, University of Notre Dame, Notre Dame, Indiana 46556

Received: October 6, 2009; Revised Manuscript Received: December 2, 2009

By employing ^1H NMR spectroscopy and molecular simulations, we provide an explanation for recent observations that the aqueous solubilities of ionic liquids exhibit salting-out to salting-in regimes upon addition of distinct inorganic salt ions. Using a typical ionic liquid [1-butyl-3-methylimidazolium bis(trifluoromethylsulfonyl)imide], we observed the existence of preferential specific interactions between the low electrical charge density (“apolar moiety”) parts of the ionic liquid cation and the inorganic salts. These a priori unexpected interactions become increasingly favorable as one moves from salting-out to salting-in effects. More specifically, this interpretation is validated by distinct aqueous solution ^1H NMR data shifts in the ionic liquid cation upon inorganic salt addition. These shifts, which are well noted in the terminal and preterminal hydrogens of the alkyl chain appended to the imidazolium ring, correlate quantitatively with solubility data, both for cases where the nature of inorganic salt is changed, at constant concentration, and for those where the concentration of a given inorganic salt is varied. Molecular simulations have also been performed permitting us to garner a broader picture of the underlying mechanism and structure of this complex solvation phenomenon. These findings can now be profitably used to anticipate solution behavior upon inorganic salt addition well beyond the specificity of the ionic liquid solutions, i.e., for a diversity of distinct solutes differing in chemical nature.

Introduction

The effect of common salts on the aqueous solubility of charged molecules such as proteins has been well described for many years.¹ The qualitative order of the ions’ salting-in or salting-out inducing ability on macromolecules is known as the Hofmeister series.¹ While this effect is phenomenologically well-established, there is a renewed interest in this subject concerning the molecular level mechanisms by which ions operate and which are still elusive and not well understood. Common knowledge usually classifies the salting-out inducing ions as “kosmotropes” while the salting-in inducing ions are typically referred to as “chaotropes”, based on their supposed ability to “create” or “destroy” the water bulk structure, as this was believed to be the central mechanism behind the Hofmeister series.^{1–4} Recent experimental data and simulation results have cast doubts on this paradigm of the change in the bulk water structure as the main phenomenon behind the effect of salts on the molecules’ aqueous solubility.^{4–10} Both experimental studies^{4–7} and molecular simulation calculations^{8–10} are converging upon the idea that ions of high charge density—with water–ion

interactions stronger than water–water interactions—are excluded from the vicinity of the solute due to their preferential hydration, decreasing the solute’s solubility in water. On the other hand, low charge density ions—with water–ion interactions weaker than water–water interactions—directly interact with the solute thus stabilizing it in water, and therefore increasing the solute’s solubility.^{11,12}

Recently, Zhang et al.¹³ proposed a model to describe the specific ion effects on the lower critical solution temperature (LCST) of the water + PNIPAM [poly(*N*-isopropylacrylamide)] + inorganic salt systems. In previous works we have successfully extended this model to the description of the solubility of ionic liquids (ILs) in aqueous salt solutions.^{11,12} Essentially, the model is based on three effects to describe the interactions between the salt ions and solutes on aqueous solutions, two of which seem to be predominant and are thus highlighted: (i) an entropic effect associated with the salting-out that results from the ability of high charge density ions to form hydration complexes away from the solute; and (ii) a direct interaction of the low charge density ions with the solute (in the case of PNIPAM, a direct interaction of the anion with the amide group was suggested¹³) that would be responsible for the salting-in. The entropic effects leading to salting-out are well supported by the experimental results reported previously.^{11–13} Evidence for the direct interaction between the ions and the solute at the basis of the salting-in phenomenon remains elusive,^{11,12} and alternative/supplementary approaches, capable of providing

* Corresponding author. Telephone: +351-234-370200. Fax: +351-234-370084. E-mail: jcoutinho@ua.pt.

[†] Universidade Nova de Lisboa.

[‡] CICECO, Departamento de Química, Universidade de Aveiro.

[§] QOPNA, Departamento de Química, Universidade de Aveiro.

^{||} Universidade do Porto.

[⊥] University of Notre Dame.

further evidence for the molecular-level interactions behind the salting-in of ILs, are still required.

Some ILs have been considered as environmentally friendly solvents due to their unique physicochemical properties.^{14–16} A special feature of these salts—among which imidazolium-based ILs have received particular attention—is that their amphiphilic character and their hydrophobicity can be tuned by varying the size of their alkyl chain length.¹⁷ Nevertheless, in spite of their growing interest, their bulk state, structure, and dynamics on a nanoscopic scale have just started being explored. Yet, based only on simplistic considerations, a structural organization in ILs and IL solutions is expected since the imidazolium cation can be sketched as a polar head with an apolar tail (the alkyl side chains). Diffraction studies^{18,19} revealed noticeable molecular organization of ILs at the nanometer scale, while molecular simulation studies^{20,21} have shown that ILs aggregate through their alkyl tails via van der Waals interactions. This local structure network feature of ILs distinguishes them from most ordinary molecular liquids and common salts. Besides some limited studies concerning aqueous solutions of ILs,^{22–24} structural investigations of their aqueous solution behavior in the presence of common inorganic ions are a particularly underexplored field.^{11,12,25–29} Nonetheless, it should be kept in mind that a molecular-based understanding of ILs is a challenging task because their electric charges, polarities, and molecular and electronic structures result in a complex interplay of molecular interactions.

In order to achieve a deeper understanding about the molecular mechanism behind the salting-in and salting-out phenomena, the solvation of the hydrophobic IL 1-butyl-3-methylimidazolium bis(trifluoromethylsulfonyl)imide ([C₄mim][Tf₂N]), commonly used as a model ionic liquid, in aqueous (D₂O) salt solutions of SO₄²⁻, CO₃²⁻, Cl⁻, and SCN⁻ with Na⁺ as cation, and Ca²⁺, Na⁺, NH₄⁺, and (CH₃)₄N⁺ with Cl⁻ as anion, is investigated in this work using ¹H NMR spectroscopy. The interpretation of the spectroscopic data is further supported by molecular dynamics simulations performed for NaCl, Na₂SO₄, and NaClO₄ aqueous solutions of [C₄mim][Tf₂N]. The cations and anions were selected to cover the entire Hofmeister series (from salting-out to salting-in inducing behaviors).¹ Both SO₄²⁻, ClO₄⁻, and SCN⁻, and Ca²⁺ and (CH₃)₄N⁺, are at the extremes of this series. Cl⁻ and Na⁺ are usually classified as almost neutral points due to their position in the middle of the series, and were used as fixed ions to investigate the influence of individual cations and anions, respectively.¹

The results here obtained provide an interesting picture of the influence of the inorganic ions on the IL solvation in aqueous solutions. As will be shown, spectroscopic and molecular simulation results support a conceptual model where the solubility of ILs in aqueous salt solutions is controlled by the interaction between the inorganic salt ions and the hydrophobic moieties of the IL: a typical ion-induced dipole interaction.

NMR Experimental Section

The specific ion effects on the IL solubility in water were studied by NMR spectroscopy for the following salts: NaCl, >99.5 w/w % pure from Panreac; NaSCN, ≥98.0 w/w % pure from Fluka; Na₂SO₄, >99.0 w/w % pure from Panreac; Na₂CO₃, >99.7 w/w % pure from Carlo Erba; NH₄Cl, >99.5 w/w % pure from Panreac; (CH₃)₄NCl, ≥98 w/w % pure from Fluka; and CaCl₂·2H₂O, >99 w/w % pure from Riedel-de Haën. All salts (ca. 1 g) were dried under reduced pressure (*p* < 1 Pa) at 323 K for at least 5 h before using, to remove water traces. The IL

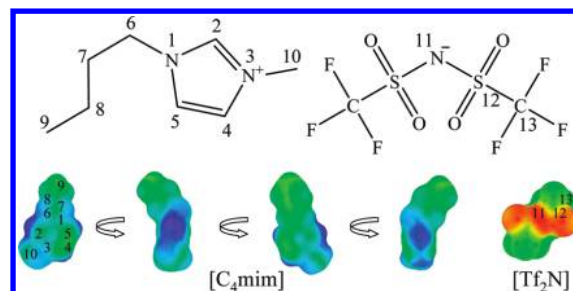


Figure 1. Chemical structure, atom numbering, and charge distribution of 1-butyl-3-methylimidazolium bis(trifluoromethylsulfonyl)imide, [C₄mim][Tf₂N].

1-butyl-3-methylimidazolium bis(trifluoromethylsulfonyl)imide, [C₄mim][Tf₂N], was from Iolitec. To reduce the water content and volatile compounds to negligible values, the IL was dried under reduced pressure (*p* < 1 Pa) at ca. 350 K using constant stirring, for a minimum of 48 h. The IL purity was further confirmed by ¹H, ¹³C, and ¹⁹F NMR spectroscopy and found to be >99 w/w %. The deuterium oxide used was acquired at Aldrich with >99.96 % D atoms. The 3-(trimethylsilyl)propionic-2,2,3,3-*d*₄ acid sodium salt (TSP) was from Aldrich with >98 % D atoms.

A solution of [C₄mim][Tf₂N] at approximately 0.012 mol·kg⁻¹ in D₂O (thus, below the IL saturation limit and sufficiently low to ensure complete dissociation in aqueous solution), using TSP as a reference, was prepared gravimetrically with an associated uncertainty of ±10⁻⁴ g. The salt solutions were further prepared gravimetrically in the D₂O–IL–TSP initial solution with salt concentrations ranging from 0 to 6.0 mol·kg⁻¹. For each salt, the IL is at the same concentration as in the pure IL–D₂O–TSP solution used as reference to determine the chemical shift deviations. Due care was taken to avoid contamination of the solutions with moisture. The ¹H NMR spectra were recorded using a Bruker Avance 300 spectrometer operating at 300.13 MHz, using D₂O as solvent and TSP as internal reference, at 298 K. Moreover, in order to distinguish the chemical shifts of H(4) and H(5) of the IL cation (Figure 1), ¹H and ¹³C NMR spectra were recorded, for the same D₂O solutions, on a Bruker Avance 500 spectrometer operating at 300.13 and 75.47 MHz, respectively. The phase sensitive ¹H-detected (¹H, ¹³C) gHSQC (heteronuclear single quantum coherence, using gradient pulses for selection) spectrum was recorded with 200 transients over 256 increments (zero-filled to 1 K) and 1 K data points with spectral widths of 3500 Hz in *F*₂ and 10 500 Hz in *F*₁. The repetition time was 2.0 s. A cosine multiplication was applied in both dimensions. The delays were adjusted according to a coupling constant ¹*J*(CH) of 149 Hz. The gHMBC (heteronuclear multiple quantum coherence, using gradient pulses for selection) spectrum was recorded with 200 transients over 256 increments (zero-filled to 1 K) and 1 K data points with spectral widths of 3500 Hz in *F*₂ and 10 500 Hz in *F*₁. The repetition time was 2.0 s. A sine multiplication was applied in both dimensions. The low-pass *J*-filter of the experiment was adjusted for an average coupling constant ¹*J*(CH) of 149 Hz, and the long-range delay utilized to excite the heteronuclear multiple quantum coherence was optimized for 7 Hz.

Molecular Dynamics Simulation Methods

In order to support the ¹H NMR chemical shift deviations observed, molecular dynamics simulations were performed for aqueous solutions of [C₄mim][Tf₂N] at 0.1 mol·dm⁻³ in the

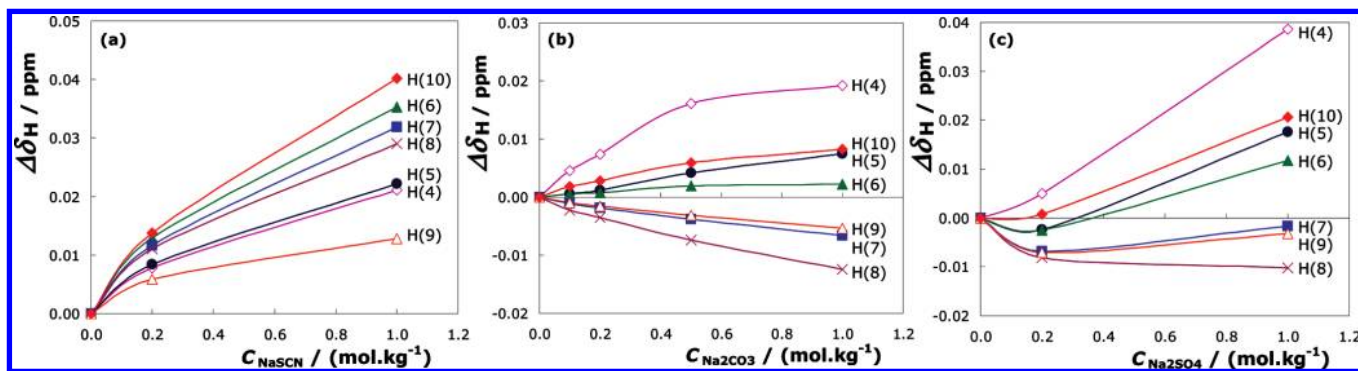


Figure 2. ^1H NMR chemical shift deviations between sodium-based salts and $[\text{C}_4\text{mim}][\text{Tf}_2\text{N}]$ in deuterated aqueous solutions and that of pure $[\text{C}_4\text{mim}][\text{Tf}_2\text{N}]$ ($0.012 \text{ mol}\cdot\text{kg}^{-1}$) in heavy water as a function of the inorganic salt molality (relative to TSP in D_2O): (a) NaSCN ; 11 (b) Na_2CO_3 ; 11 (c) Na_2SO_4 .

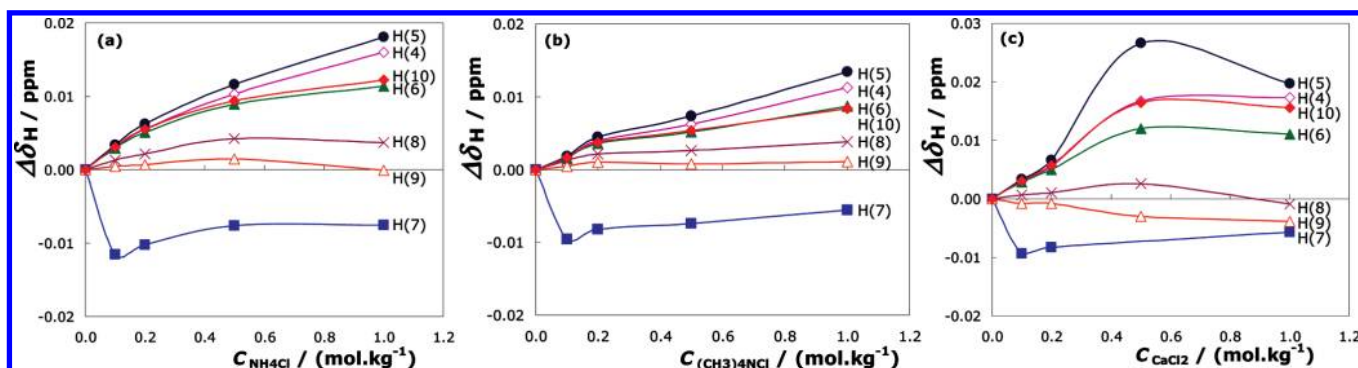


Figure 3. ^1H NMR chemical shift deviations between chloride-based salts and $[\text{C}_4\text{mim}][\text{Tf}_2\text{N}]$ in deuterated aqueous solutions and that of pure $[\text{C}_4\text{mim}][\text{Tf}_2\text{N}]$ ($0.012 \text{ mol}\cdot\text{kg}^{-1}$) in heavy water as a function of the inorganic salt molality (relative to TSP in D_2O): (a) NH_4Cl ; (b) $(\text{CH}_3)_4\text{NCl}$; (c) CaCl_2 .

presence of three additional salts: NaCl , Na_2SO_4 , and NaClO_4 . For NaCl , three concentrations (0.20 , 1.0 , and $2.0 \text{ mol}\cdot\text{dm}^{-3}$) that exhibited experimental salting-in and salting-out of the IL were selected. For Na_2SO_4 , concentrations of 0.20 and $1.0 \text{ mol}\cdot\text{dm}^{-3}$ were chosen, while three concentrations (0.20 , 1.0 , and $2.0 \text{ mol}\cdot\text{dm}^{-3}$) were studied for NaClO_4 .

Molecular dynamics simulations were carried out in the canonical (NVT) ensemble using the program NAMD 2.6. 30 The simple point charge (SPC) model parameters were used for the van der Waals and electrostatic parameters for water. 31 Harmonic force constants for bond vibrations and angle bending were set to $450 \text{ kcal}\cdot\text{mol}^{-1}\cdot\text{\AA}^{-2}$ and $55.0 \text{ kcal}\cdot\text{mol}^{-1}\cdot\text{rad}^{-2}$, respectively. 32 Force field parameters for the IL cation were obtained from the work of Cadena and Maginn, 33 while those for the IL anion were taken from those developed by Canongia Lopes and Pádua. 34 Lennard-Jones parameters for Na^+ and Cl^- were taken from Jensen and Jorgensen, 35 while those for SO_4^{2-} were from the work of Cannon et al. 36 In the absence of a force field for SCN^- , an equivalent salting-out anion was studied, namely ClO_4^- , whose parameters were obtained from the work of Cadena and Maginn. 33

Simulations were conducted at 298.15 K using a Langevin thermostat applied to all heavy atoms. The damping coefficient of the temperature bath was set to 1 ps^{-1} . Nonbonded interactions were truncated at 12.0 \AA by smoothly varying the potential from 10 \AA . Electrostatic interactions were calculated with the particle mesh Ewald method with a grid spacing of $\sim 1.0 \text{ \AA}$. The equations of motion were integrated with a 1 fs time step, and trajectories were saved every 500 fs for radial distribution analysis.

Starting configurations were generated in a cubic simulation box of dimensions $40 \text{ \AA} \times 40 \text{ \AA} \times 40 \text{ \AA}$. The density of water

at 298.15 K ($0.997 \text{ g}\cdot\text{cm}^{-3}$) was used to determine the number of water molecules used. Based on this, four IL cation–anion pairs were included to arrive at the IL concentration of $0.1 \text{ mol}\cdot\text{dm}^{-3}$. For various salt concentrations, the number of cation–anion pairs was determined in a similar manner. The system was prepared by randomly placing water molecules and ions in the simulation box. This was followed by a 1000 step steepest-descent minimization to alleviate high-energy overlap. The system was heated to 298.15 K by incrementing the temperature in intervals of 50 K . During each interval, the system was simulated for 5 ps in the NVT ensemble. The final simulation at 298.15 K was performed for 5 ns , out of which the last 4 ns of data was used for later analysis.

Results and Discussion

NMR Spectroscopy. The chemical structure, atom numbering, and charge distribution for the studied IL are depicted in Figure 1. The surface of an IL is usually composed of hydrophobic (signed as green) and hydrophilic moieties including local charges (positive distribution charge signed as blue and negative distribution charge illustrated as orange–yellow). The number of carbon atoms at the longer alkyl chain is the main factor determining the hydrophobic nature of the studied IL cation, and as will be shown below, the hydrophobic hydration of the IL alkyl chain in the presence of salt ions controls its solubility behavior in aqueous solution.

Figures 2 and 3 present, respectively, the ^1H NMR chemical shift deviations for the sodium-based and the chloride-based salt solutions as a function of the salt concentration, while Figure 4 depicts the chemical shift deviations obtained for the aqueous NaCl solutions (cf. Supporting Information with the ^1H NMR

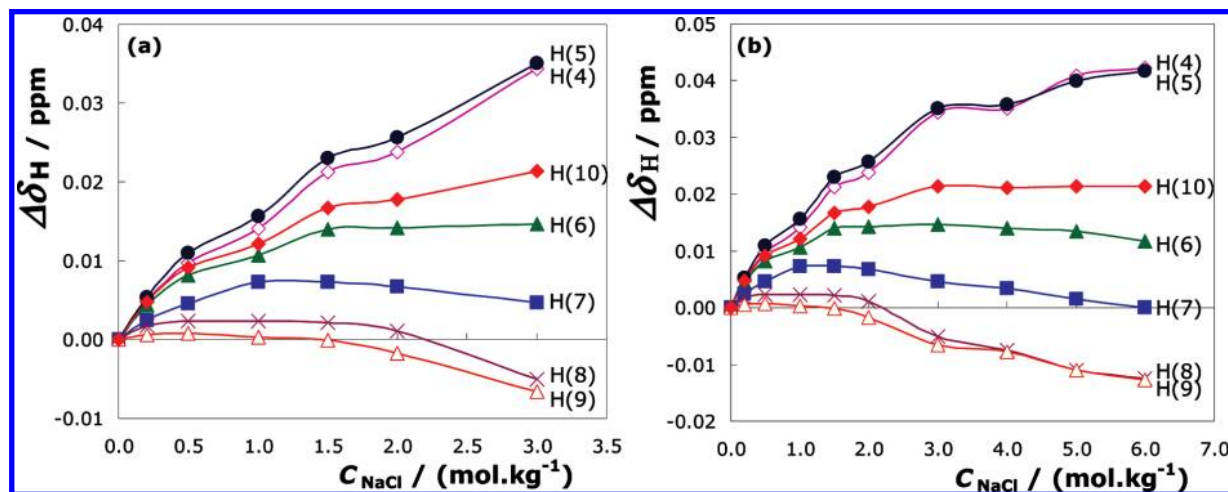


Figure 4. ^1H NMR chemical shift deviations between NaCl and $[\text{C}_4\text{mim}][\text{Tf}_2\text{N}]$ in deuterated aqueous solutions and that of pure $[\text{C}_4\text{mim}][\text{Tf}_2\text{N}]$ ($0.012 \text{ mol}\cdot\text{kg}^{-1}$) in heavy water as a function of the NaCl molality (relative to TSP in D_2O): (a) up to $3.0 \text{ mol}\cdot\text{kg}^{-1}$ of NaCl; (b) up to $6.0 \text{ mol}\cdot\text{kg}^{-1}$ of NaCl.

chemical shifts). The ^1H NMR chemical shift deviations are defined according to eq 1

$$\Delta\delta_{\text{H}} = \delta_{\text{H(IL+salt)}} - \delta_{\text{H(IL)}} \quad (1)$$

where $\delta_{\text{H(IL+salt)}}$ are the ^1H NMR chemical shifts of the IL deuterated solution in the presence of inorganic salts and $\delta_{\text{H(IL)}}$ are the ^1H NMR chemical shifts of the pure deuterated IL solution.

It has been noticed previously that the chemical shifts of the imidazolium ring protons are both anion and concentration dependent with the highest differences observed at the C(2) proton (the most acidic hydrogen at the aromatic ring).³⁷ Two different phenomena were proposed to explain the chemical shift deviations: hydrogen bonding and ring π -stacking.³⁷ However, in this work, the chemical shift deviations are always reported in relation to the pure IL– D_2O –TSP solution, maintaining the same IL concentration in the salt aqueous solutions, thus avoiding such chemical shift deviations.

The acidic proton at C(2), located between the two N atoms at the imidazolium ring, is capable of hydrogen bonding with the IL counteranion in the pure state.³⁸ It has been argued that this interaction leads to significant anion–cation pair formation with concomitant loss of the IL ionic character.³⁸ Although an important interaction between H(2) and the salt ions was expected, the signal of H(2) does not appear in any of the ^1H NMR spectra. This is believed to be caused by the exchange of this acidic hydrogen with deuterium afforded by the solvent.

It has been previously shown³⁷ that the alkyl chain protons of the IL cation are quite insensitive to interactions with the IL anion, while the H(2), H(4), and H(5) protons are the major sites for interactions with the anion. In this work, we have confirmed that favorable interactions between the salt ions and the polar/charged moiety of the molecule (protons H(4), H(5), H(6), and H(10)) are always present (Figures 2–4). However, we have found a remarkable interaction, not previously noticed, between the inorganic salt ions and the terminal protons of the longest alkyl chain of $[\text{C}_4\text{mim}][\text{Tf}_2\text{N}]$. In Figures 3 and 4 it is possible to observe favorable interactions (positive deviations) between the salting-in inducing ions (SCN^- , NH_4^+ , and $(\text{CH}_3)_4\text{N}^+$) and the terminal protons of the hydrophobic alkyl chain (H(8) and H(9)). This interaction is conspicuously absent for the salting-out inducing ions. In addition, for SCN^- , positive

interactions with H(7) are also observed. While for the salting-in inorganic cations such interactions occur for H(8) and H(9), for the inorganic anions they are more widespread with favorable interactions with H(7), H(8), and H(9). This tendency derives from the fact that anions are typically more polarizable than cations due to their more diffuse valence electronic configuration and, therefore, their salting-in/-out effects are thus more pronounced.

Besides this new general observation that favorable interactions between terminal alkyl chain protons and salting-in inducing ions exist (an absent feature for the salting-out inducing ions), the behavior of the NaCl solutions, reported in Figure 4, is particularly remarkable: salting-in effect at low inorganic salt concentrations followed by salting-out at higher salt concentrations.¹¹ Here, the observed ^1H NMR chemical shift deviations of H(8) and H(9) explain this solubility turnover as they also follow this trend, thus suggesting that the favorable interactions of the salt ions with these protons are responsible for the initial IL salting-in, followed by salting-out as the interactions become less favorable. This trend in solubility is analogous to what is observed for the aqueous solubility of other charged molecules, such as amino acids and proteins.³⁹ Suggestions from other authors that the salting-in phenomenon could result from favorable interactions between the inorganic salt ions and the hydrophobic moieties of the solute have already been reported,^{9,10} although experimental evidence to support that idea has only recently been obtained by our group.^{11,12} We have found that ^1H NMR spectra provide clear experimental evidence for the underlying molecular mechanism responsible for salting-in based on the presence and intensity of favorable interactions between the salt ions and the hydrophobic moiety of the solute.

A further remarkable point concerning the ^1H NMR data is that the magnitude of ^1H NMR chemical shift deviations, for the terminal and preterminal protons in the alkyl chain (H(7), H(8), and H(9)), clearly correlate with the IL solubility trend previously reported.¹¹ The dependency of the aqueous solubility of IL in pure water compared to that in the presence of salt with the chemical shift deviations for protons H(7), H(8), and H(9) is shown in Figure 5, for the sodium-based salts. Note that no correlation was found for the other protons present at the imidazolium cation.

The picture that can be drawn from the ^1H NMR spectra is that the salt ions have always favorable interactions with the polar/charged region of the IL cation. Moreover, the salting-

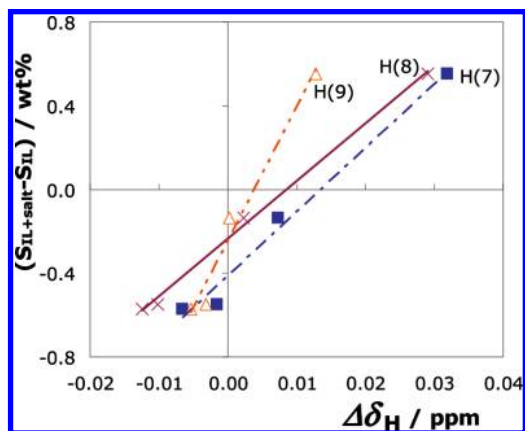


Figure 5. Relative deviation in the solubility of [C₄mim][Tf₂N] in aqueous salt solutions (at 1.0 mol·kg⁻¹) from that in pure water and its dependence on the ¹H NMR chemical shift deviations for the imidazolium cation protons H(7), H(8), and H(9).

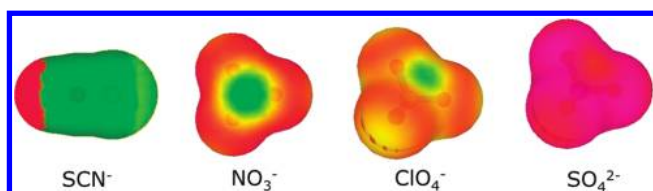


Figure 6. Charge distribution for inorganic anions ordered from salting-in to salting-out effects.

out inducing ions display nonfavorable interactions with the IL nonpolar regions, suggesting that the former have higher affinity for water than for the IL long alkyl chain, and thus, their solvation will reduce the hydrophobic hydration of the IL cation. Conversely, favorable direct interactions between the salting-in inducing ions and the hydrophobic part of the IL cation are observed, suggesting that the favorable adsorption of these ions to hydrophobic surfaces^{9,10} confers on them characteristics that enhance the solubility of the solute in aqueous solutions. Note that ions at the salting-in extreme of the Hofmeister series are ions such as thiocyanate, perchlorate, nitrate, ammonium, or, in the limit, some halogenates (Cl⁻ and Br⁻). For most of these ions the charge is highly dispersed, so they can interact with the hydrophobic surfaces/moieties of the solutes via interactions such as ion-induced dipole or even dispersion forces. The charge distribution of some inorganic anions ordered from salting-in to salting-out effects is shown in Figure 6 for a clearer perspective of the phenomenon. For the salting-in anions it is visible that the negative charge is well dispersed (hence, shown in orange–yellow) with additional nonpolar domains (shown in green). In contrast, for salting-out anions the negative charge is highly localized (marked as pink–red). Obviously the same analogy can be rationalized for the inorganic salt cations. Therefore, in summary, ¹H NMR spectroscopy results have revealed a direct, specific binding of inorganic salt ions presenting moderately high charge density with the hydrophobic moiety of a molecule (ion-induced dipole interactions), an interaction that becomes increasingly favorable as one moves from salting-out to salting-in effects.

There are, nevertheless, some interesting consequences of the salting-in mechanism that can be tested in future work or confirmed by experimental literature data for other systems. Unlike the salting-out effect, where the interactions of salt ions with water seem to be dominant, for the salting-in the interactions between the salt and the solute control the solubility. Thus, the salting-out effect is more solute independent than the salting-

in. An ion that is able to salt-in some solutes may have a salting-out effect with others, e.g., hexafluorobenzene solubility in aqueous NaNO₃ solutions.⁴⁰ In this case, the NO₃⁻ anion, usually a salting-in inducing ion, has an interaction with a completely fluorinated solute that is not favorable and the preferential hydration of the inorganic salt ions occurs, leading to salting-out of hexafluorobenzene. Since in most cases the interactions leading to the salting-in phenomenon will take place between inorganic salts and alkyl chains, one should expect, in some cases, solute-independent effects. However, if the added salt is not a simple inorganic salt but is instead, e.g., a quaternary ammonium, a guanidinium, or one derived form of an amino acid, then the interactions between the solute and the salt will certainly be of a more complex nature.

Nonetheless, there are a number of questions that the study of the chemical shifts of the ¹H NMR spectra leaves unanswered: What about the solvation of the IL anion by the inorganic salt ions? How are the relative adsorptions of the inorganic salt anion and cation to the IL ions? Will both contribute to the salting-in, or will they have different influences upon the solute solubility? To obtain clues to these and other questions, we have been assisted by molecular dynamics simulations which provide us with a more complete, albeit modeled, picture of the molecular level interactions occurring on these systems and of the distribution of the ions around the solute.

Molecular Dynamics Simulation. Radial distribution functions (RDFs), denoted by $g(r)$, were calculated from the molecular dynamics trajectories and analyzed to obtain further insights into the organization of salt ions around the IL cation and anion. These distributions provide a quantitative description of enhancement ($g(r) > 1$) or depletion ($g(r) < 1$) of densities of species around a selected moiety.

The first interesting results are the RDFs of water around the IL ions. The RDFs around the alkyl moieties of the cation show a depletion in water density at approximately 6–7 Å consistent with their hydrophobic nature. Similarly, water densities around the IL anion exhibit no structuring. Particularly remarkable is that the RDFs are essentially identical for all the alkyl moieties of the IL cation in the three salts studied; cf. Supporting Information. This is a strong argument against the classical interpretation of the salting-in/-out as resulting from a change in the water structure. The RDFs clearly indicate that the water structure around the solute is not affected by the different salts present in solution, implying that the salting-in/-out behavior of ILs by different salts does not depend on the structure of water around the solute ions.

The RDFs of Na show the absence of Na in the first hydration layer of the IL cation. On the other hand, the RDFs of Na with the IL anion show a strong interaction, particularly with the oxygen atoms of the sulfonyl groups. The interaction of Na and the IL anion decreases as the NaCl concentration increases, thus favoring the salting-out of the IL with increasing NaCl concentration; cf. Supporting Information. Some ordering of Na around the charged nitrogen atom of the anion is also observed, although, when compared with the ordering around the anion oxygen atoms, it is weak and only occurs at the second solvation layer. For Na₂SO₄, a similar ordering of Na around the oxygen and nitrogen atoms of the IL anion is also observed, even though the peaks are less intense, thus suggesting a weaker binding of Na with the IL anion when SO₄²⁻ is the counteranion; cf. Supporting Information. In contrast to NaCl and Na₂SO₄, RDFs of Na for the NaClO₄ system reveal enhanced ordering of Na around both oxygen and nitrogen atoms of the anion. Moreover, the intensity of the first and second solvation shell peaks

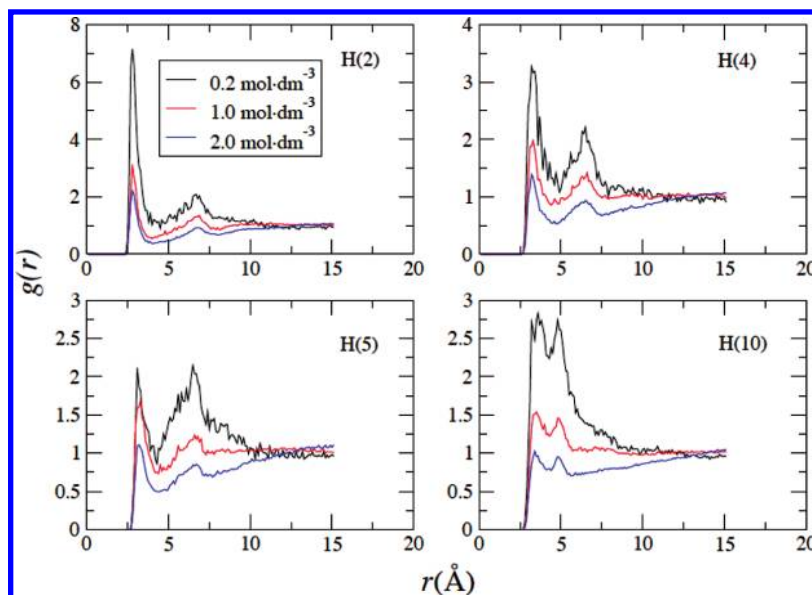


Figure 7. Radial distribution functions of Cl from NaCl with H(2), H(4), H(5), and H(10).

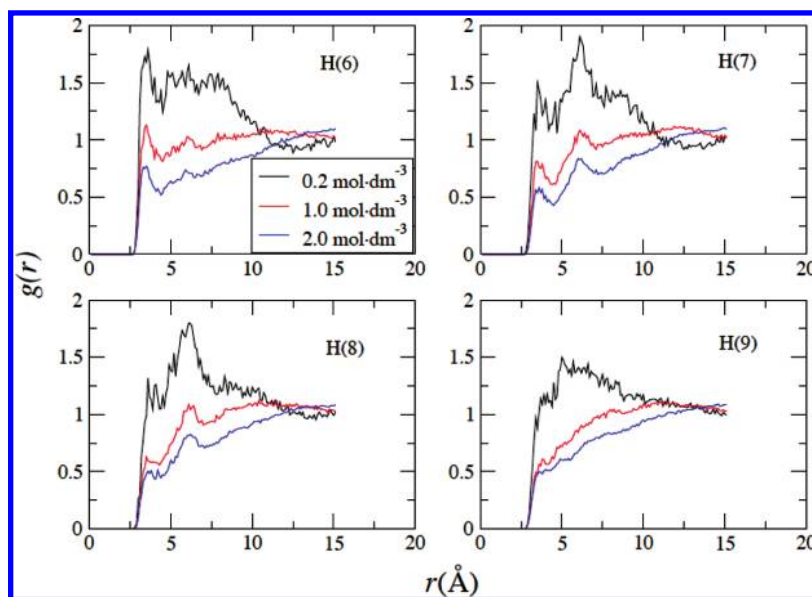


Figure 8. Radial distribution functions of Cl from NaCl with H(6), H(7), H(8), and H(9).

increases with higher concentrations of NaClO_4 . This observation suggests that direct interaction of Na with the IL anion contributes to the intrinsic salting-in ability of NaClO_4 ; cf. Supporting Information.

As expected, the ordering of the inorganic anions around the IL anion is weaker than the ordering observed for the salt cations around the IL anion; cf. Supporting Information. Nevertheless, the RDFs suggest the presence of a slight ordering of Cl around the atoms F and O composing the IL anion which indicates the presence of a minor, yet still favorable, interaction taking place. Note that these interactions are absent in SO_4^{2-} systems. In contrast to these observations, the RDF of Cl in ClO_4^- around F exhibits an increase in the first peak intensity with increasing salt concentration, suggestive of ordering of the salt anion. The presence of the inorganic salt anion around the IL anion is related to the proximity of the IL anion to the alkyl hydrogen groups of the IL cation, where clustering of ClO_4^- is observed (see below). The increase in peak intensity in the second solvation shell observed in the N–Cl RDF is due to the association of ClO_4^- around F of the IL anion.

RDFs for Cl around $[\text{C}_4\text{mim}]^+$, reported in Figures 7 and 8, show that the localization of Cl is dominant around H(2) as indicated by the intensity of the peak for the first hydration layer. These results are in full agreement with what is known about the charge distribution on the IL cation as displayed in Figure 1. Interactions with the protons H(4) and H(5), albeit less intense than with H(2), are also observed and are in agreement with the ^1H NMR chemical shift deviations.

The most interesting and unexpected results were obtained for the RDFs of salt anions and the IL cation protons H(6), H(7), H(8), and H(9). Figure 8 shows the interaction between Cl and the alkyl chain protons. Although the peak intensity is less than that observed with the charged protons close to the aromatic ring, there is nevertheless a clear and intense presence of the chloride ions in the first solvation layer of the alkyl chains, which decreases with increasing salt concentration.

As is the case with the NaCl solution, RDFs for the Cl atom in ClO_4^- indicate organization of the anion around the IL aromatic hydrogens (H(2), H(4), H(5)). Also, as observed for the NaCl, the intensity of the first peak in the RDF decreases

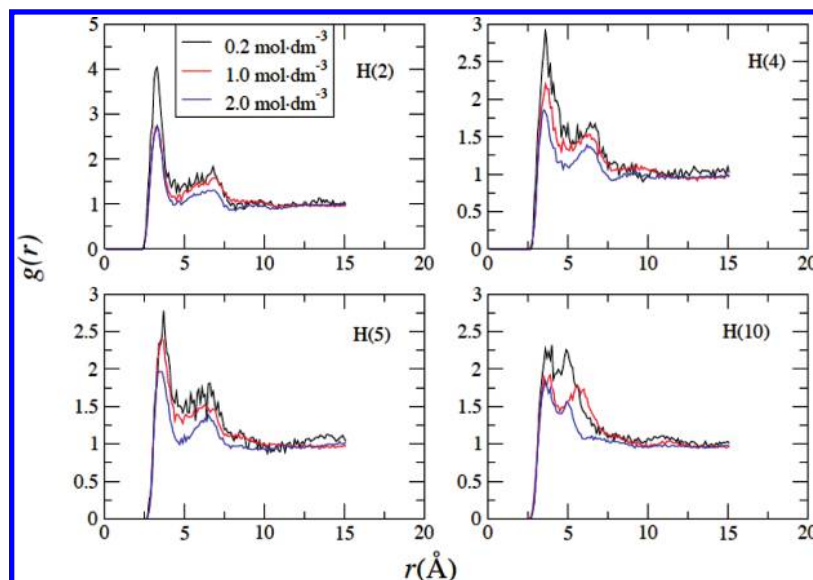


Figure 9. Radial distribution functions of Cl from NaClO₄ with H(2), H(4), H(5), and H(10).

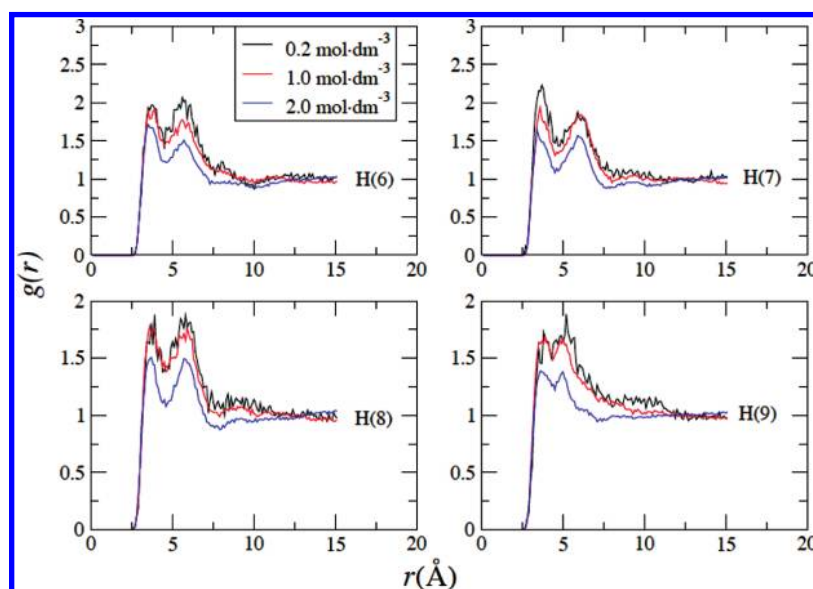


Figure 10. Radial distribution functions of Cl from NaClO₄ with H(6), H(7), H(8), and H(9).

with increasing salt concentration. In contrast to NaCl solutions, however, the reduction in peak intensity is significantly less remarkable in ClO₄⁻. It is evident from Figures 9 and 10 that association of ClO₄⁻ with the IL cation persists over the entire range of concentrations studied. RDFs of the salt anion around H(6), H(7), H(8), and H(9) in the IL cation are in stark contrast to those obtained for Cl⁻ and SO₄²⁻ discussed below. The RDFs show that ClO₄⁻ interacts strongly with the alkyl tails of the IL cation, as shown by the ordering in the first and second solvation shells of H(6), H(7), H(8), and H(9). The intensity of the first solvation peak is comparable to that observed for the imidazolium ring hydrogen atoms. The intensity of the peaks shows little decrease with increasing salt concentration. This is in good agreement with the results for the ¹H NMR chemical shift deviations for salting-in inducing ions, supporting the hypothesis that the salting-in effect is due to direct binding of the salt anions with the hydrophobic moieties of the IL cation. In addition to the direct association of inorganic salt anions at the hydrophobic interface of the IL, analysis of RDFs of inorganic ions around the IL anion reveals the possibility of an interaction of the salt ions with the IL anion as contributing to the salting-in behavior.

Unlike what was observed for ClO₄⁻ and Cl⁻, the RDFs of SO₄²⁻ around the IL cation, presented in Figures 11 and 12, do not reveal any ordering or even the presence of SO₄²⁻ in the first solvation layer of the IL alkyl chain (H(6) to H(10) protons). A minor presence of SO₄²⁻ around the charged ring protons H(2) and H(4) is nevertheless observed. These distinct structural organizations displayed differently by salting-in and salting-out ions are properly illustrated in Figure 13. The salting-out SO₄ anion does not associate to an appreciable extent with the hydrophobic tail of the [C₄mim] cation, while the salting-in ClO₄ anion clearly clusters near the hydrophobic alkyl tail. This difference in behavior between SO₄²⁻ and Cl⁻ and ClO₄⁻, in particular in what concerns the interactions with the protons of the IL cation alkyl chain, and also to a much lower extent with the IL anion, is parallel to what is observed in the ¹H NMR chemical shift deviations and in the solubility behavior of the IL in the presence of such salts in aqueous solution.

The molecular dynamics results suggest that the ranking of salting-out to salting-in inducing ability goes as SO₄²⁻ < Cl⁻ < ClO₄⁻, a trend that is similar to the ranking in the Hofmeister

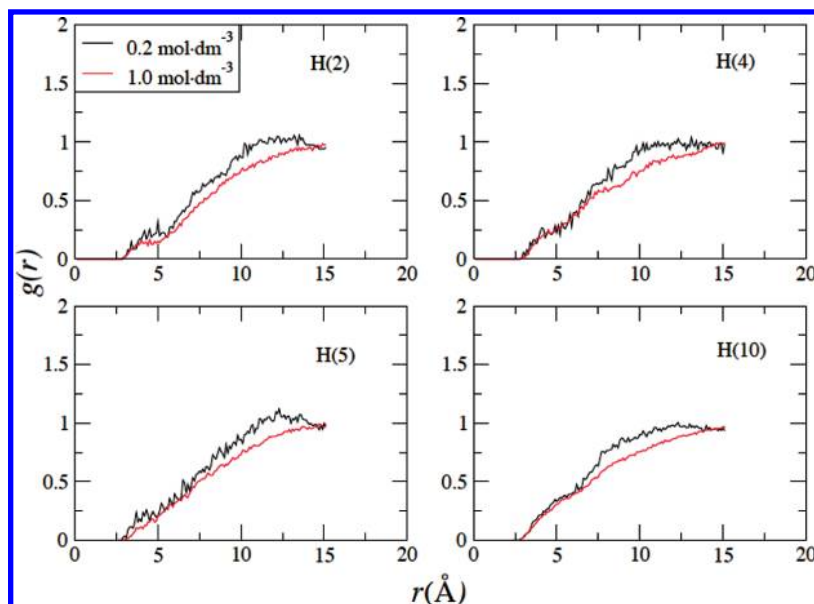


Figure 11. Radial distribution functions of S from Na₂SO₄ with H(2), H(4), H(5), and H(10).

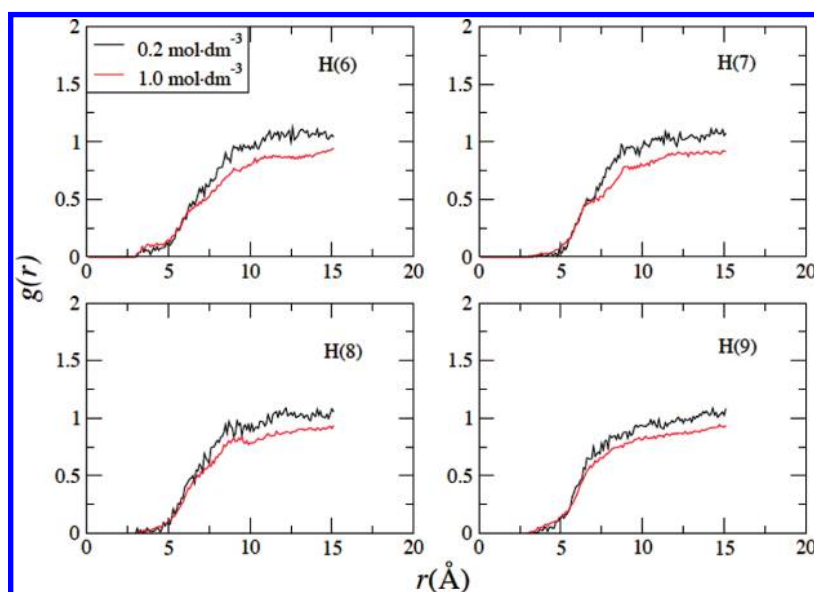


Figure 12. Radial distribution functions of S from Na₂SO₄ with H(6), H(7), H(8), and H(9).

series for anions and as also previously established experimentally for these systems.¹¹

To quantify the salting-in and salting-out effects of the IL by different salts, a thermodynamic approach based on Kirkwood–Buff (KB)^{36,41} theory was investigated. For the present case, species 1 is the aqueous solvent, species 2 is the IL solute, and species 3 is the inorganic salt. In the KB formalism, the derivative of the solute excess chemical potential (μ_2^{ex}) with respect to the change in concentration of the salt (ρ_3) in the solvent is given by^{41,42}

$$-\frac{1}{k_B T} \left(\frac{\partial \mu_2^{\text{ex}}}{\partial \ln \rho_3} \right) = \frac{\rho_3 (G_{23} - G_{21})}{1 + \rho_3 (G_{33} - G_{31})} \quad (2)$$

where the numerator on the right-hand side is a preferential interaction parameter, $\Gamma_{23} = \rho_3 (G_{23} - G_{21})$, and indicates the degree to which the local concentration of salt is enhanced over that of the bulk concentration. Γ_{23} accounts for contributions

of both local enhancements and changes in more distant solvation shells. G_{ij} represents the KB integral for a given pair $i-j$ and is given by

$$G_{ij} = \int_0^{\infty} 4\pi R^2 (g_{ij}(R) - 1) dR \quad (3)$$

where g_{ij} is the radial distribution function of the pair $i-j$. The KB integral is defined for the grand canonical ensemble. However, for closed ensembles (canonical and isothermal–isobaric), it can be approximated as^{42,43}

$$G_{ij} \approx \int_0^{R_c} 4\pi R^2 (g_{ij}^{\text{NVT}}(R) - 1) dR \quad (4)$$

where R_c is the distance at which the KB integral is truncated. This approach provides a reasonable approximation to eq 2 as long as the cutoff distance is chosen to be not too close to half the simulation box length. In this study, the KB integral is

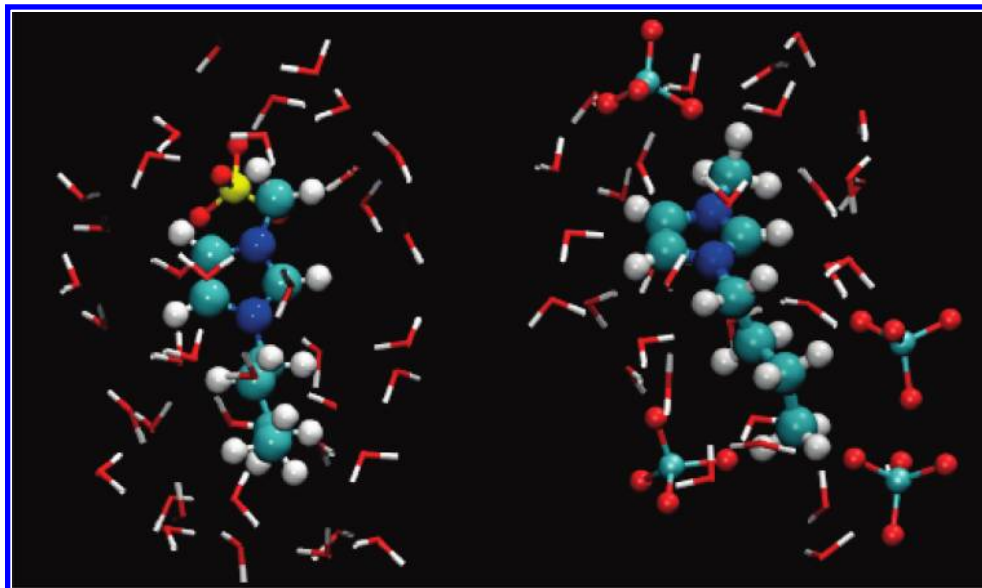


Figure 13. Snapshots from molecular dynamics simulations of $[C_4mim][Tf_2N]$ with a Na_2SO_4 solution (left) and a $NaClO_4$ solution (right).

TABLE 1: Radial Distribution Functions Computed for Evaluation of the KB Integrals in eq 2

KB integral	radial distribution functions ^a
G_{21}	IL cation–COM–OW IL anion–COM–OW
G_{23}	IL cation–COM–salt cation IL cation–COM–salt anion L anion–COM–salt cation IL anion–COM–salt anion
G_{33}	salt cation–salt cation salt anion–salt anion salt cation–salt anion
G_{31}	salt cation–OW salt anion–OW

^a COM, center of mass; OW, oxygen site in water.

mapped out as a function of the cutoff distance to draw inferences regarding the behavior of excess chemical potential of the IL as a function of salt concentration.

Since the KB theory places no restrictions on the choice of molecular centers to compute the radial distribution function

g_{ij} , for simplicity, the molecular center of mass was chosen to provide a good description of the IL cation and anion. In the case of salts, sodium was always represented as an interaction site while Cl and S were used as sites for the anions in NaCl, $NaClO_4$, and Na_2SO_4 , respectively. Radial distribution functions with water were calculated based on the oxygen atom of the molecule.

When applying the KB theory to ionic solutes and ionic cosolvents, caution must be exercised so as to not violate the electroneutrality condition.^{42,44} This amounts to the assumption that the dissociated ions are indistinguishable and leads to the transformation of systems containing five species (water, salt cation, salt anion, IL cation, and IL anion) into a ternary system comprised only of water, salt, and IL. Thus the densities of salt and IL used in eq 2 are given by the sum of densities of individual ions.^{42,44} In this formalism, various distribution functions required to calculate the KB integrals in eq 2 are provided in Table 1.

The preferential interaction parameters were calculated for all the solutions at their highest salt concentrations and are

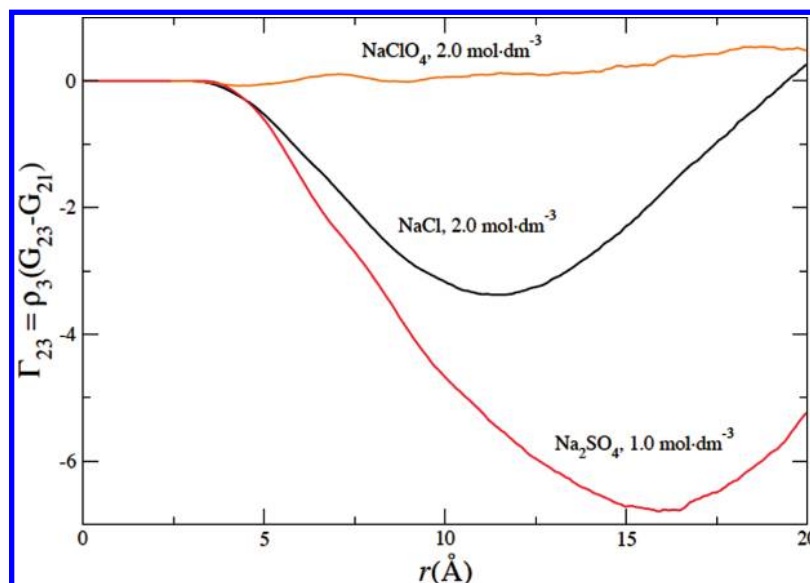


Figure 14. Preferential interaction parameter of $[C_4mim][Tf_2N]$ in $2.0 \text{ mol}\cdot\text{dm}^{-3}$ NaCl, $1.0 \text{ mol}\cdot\text{dm}^{-3}$ Na_2SO_4 , and $2.0 \text{ mol}\cdot\text{dm}^{-3}$ $NaClO_4$.

displayed in Figure 14 as a function of distance. The numerical value of the interaction parameter varies as a function of the cutoff distance. However, it is clear that the parameter is positive for NaClO₄ for $R > 5 \text{ \AA}$ while for NaCl and Na₂SO₄ it is negative at all distances (except at half the box dimension, where the approximation embedded in eq 2 breaks down). The positive values of Γ_{23} for ClO₄⁻ suggest enhancement of salt concentration relative to water in the vicinity of IL ions, which is in agreement with the qualitative analysis of the ClO₄⁻ RDFs.

Since the denominator in eq 2 was found to be positive (cf. Supporting Information) for all the salt systems, it indicates that the solute excess chemical potential decreases with positive values of Γ_{23} as observed for NaClO₄, which implies salting-in behavior for the IL. On the other hand, negative values of the preferential interaction parameter suggest an increase in the solute excess chemical potential leading to a salting-out effect. It is clear that, for NaCl and Na₂SO₄, KB theory predicts salting-out phenomena for the IL with increasing concentration of the salts. This is also confirmed by the radial distribution analysis presented earlier for these salt solutions. It is also worth noting that the excess chemical potential of IL is predicted to increase at a much faster rate in the case of Na₂SO₄ compared to that in NaCl, implying that the former is much stronger salting-out agent than the latter, which is consistent with experimental observations.

Conclusions

This work provides some novel and important insights into the nature of the Hofmeister series using a relatively new substance—an ionic liquid. Both by ¹H NMR spectroscopy and molecular simulations, we provide a thorough explanation for recent observations that the aqueous solubilities of ILs exhibit changes from salting-out to salting-in regimes upon the addition of distinct inorganic salt ions. Quantitative correlations have been observed between the measured ¹H NMR chemical shifts as inorganic salts are added to the solution and the solubilities of ILs in those aqueous salt solutions. Moreover, molecular simulations have also been performed permitting us to garner a deeper and broader picture of the underlying mechanism and structure of this complex solvation phenomenon.

The effect of single ions on the aqueous solubility of charged molecules has long been qualitatively well described by the Hofmeister series, yet the molecular level mechanisms by which ions operate is still not fully understood. This work shows that the controlling interactions that determine the salting-in phenomena in large charged molecules take place between the salt ions and the hydrophobic moiety of the solute as clearly revealed by the ¹H NMR spectra and the molecular simulations. These are some of the first evidence for the direct interaction of inorganic salt ions presenting low charge density with the hydrophobic moiety of a molecule, an interaction that, as shown here, becomes increasingly favorable as one moves from salting-out to salting-in effects. Interactions of ions with hydrophobic surfaces may appear quite exotic, but it should be noticed that the ions at the salting-in extreme of the Hofmeister series are either complex cations such as quaternary ammoniums and guanidiniums, or anions such as thiocyanate, perchlorate, or, in the limit, some halogenates (Cl⁻ and Br⁻). For most of these ions the charge is highly dispersed, so they can associate with the hydrophobic surfaces/moieties of the solutes via nonelectrostatic interactions such as ion-induced dipole or even dispersion forces. It is here shown that it is this favorable ion-solute interaction which contributes to the increase in solubility of hydrophobic compounds in aqueous solutions.

The link of this unexpected finding to the salting-in effect induced by salts in the aqueous solubility of other complex molecules is straightforward and of high relevance.

Acknowledgment. The authors thank FCT for Project PTDC/EQU-FTT/65252/2006 and Grant SFRH/BPD/41781/2007. E.J.M. and J.K.S. acknowledge support from the Air Force Office of Scientific Research under Contract No. FA9550-07-1-0443.

Supporting Information Available: ¹H NMR chemical shifts (A) and molecular dynamics simulation (B) results. This material is available free of charge via the Internet at <http://pubs.acs.org>.

References and Notes

- Hofmeister, F. *Arch. Exp. Pathol. Pharmacol.* **1888**, XXV, 1.
- Collins, K. D.; Washbaugh, M. W. *Q. Rev. Biophys.* **1985**, 18, 323.
- Caçace, M. G.; Landau, E. M.; Ramsden, J. J. *Q. Rev. Biophys.* **1997**, 30, 241.
- Holz, M.; Grunder, R.; Sacco, A.; Meleleo, A. *J. Chem. Soc., Faraday Trans.* **1993**, 89, 1215.
- Holz, M. *J. Mol. Liq.* **1995**, 67, 175.
- Sacco, A.; De Cillis, F. M.; Holz, M. *J. Chem. Soc., Faraday Trans.* **1998**, 94, 2089.
- Westh, P.; Kato, H.; Nitshikawa, K.; Koga, Y. *J. Phys. Chem. A* **2006**, 110, 2072.
- Kalra, A.; Tugcu, N.; Cramer, S. M.; Garde, S. *J. Phys. Chem. B* **2001**, 105, 6380.
- Zangi, R.; Berne, B. J. *J. Phys. Chem. B* **2006**, 110, 22736.
- Zangi, R.; Hagen, M.; Berne, B. J. *J. Am. Chem. Soc.* **2007**, 129, 4678.
- Freire, M. G.; Carvalho, P. J.; Silva, A. M. S.; Santos, L. M. N. B. F.; Rebelo, L. P. N.; Marrucho, I. M.; Coutinho, J. A. P. *J. Phys. Chem. B* **2009**, 113, 202.
- Tomé, L. I. N.; Varanda, F. R.; Freire, M. G.; Marrucho, I. M.; Coutinho, J. A. P. *J. Phys. Chem. B* **2009**, 113, 2815.
- Zhang, Y.; Furyk, S.; Bergbreiter, D. E.; Cremer, P. S. *J. Am. Chem. Soc.* **2005**, 127, 14505.
- Holbrey, J. D.; Seddon, K. R. *Clean Prod. Processes* **1999**, 1, 223.
- Earle, M. J.; Esperança, J. M. S. S.; Gilea, M. A.; Lopes, J. N. C.; Rebelo, L. P. N.; Magee, J. W.; Seddon, K. R.; Widegren, J. A. *Nature* **2006**, 439, 831.
- Santos, L. M. N. B. F.; Canongia Lopes, J. N.; Coutinho, J. A. P.; Esperança, J. M. S. S.; Gomes, L. R.; Marrucho, I. M.; Rebelo, L. P. N. *J. Am. Chem. Soc.* **2007**, 129, 284.
- Blesic, M.; Marques, M. H.; Plechkova, N. V.; Seddon, K. R.; Rebelo, L. P. N.; Lopes, A. *Green Chem.* **2007**, 9, 481.
- Hardacre, C.; Holbrey, J. D.; McMath, S. E. J.; Bowron, D. T.; Soper, A. K. *J. Chem. Phys.* **2003**, 118, 273.
- Triolo, A.; Mandanici, A.; Russina, O.; Rodriguez-Mora, V.; Cutroni, M.; Hardacre, C.; Bleif, H.-J.; Keller, L.; Ramos, M. A. *J. Phys. Chem. B* **2006**, 110, 21357.
- Wang, Y.; Voth, G. A. *J. Am. Chem. Soc.* **2005**, 127, 12192.
- Canongia Lopes, J. N. A.; Pádua, A. A. H. *J. Phys. Chem. B* **2006**, 110, 3330.
- Freire, M. G.; Carvalho, P. J.; Gardas, R. L.; Marrucho, I. M.; Santos, L. M. N. B. F.; Coutinho, J. A. P. *J. Phys. Chem. B* **2008**, 112, 1604.
- Freire, M. G.; Neves, C. M. S. S.; Carvalho, P. J.; Gardas, R. L.; Fernandes, A. M.; Marrucho, I. M.; Santos, L. M. N. B. F.; Coutinho, J. A. P. *J. Phys. Chem. B* **2007**, 111, 13082.
- Najdanovic-Visak, V.; Esperança, J. M. S. S.; Rebelo, L. P. N.; Ponte, M. N.; Guedes, H. J. R.; Seddon, K. R.; Szydowski, J. *J. Phys. Chem. Chem. Phys.* **2002**, 4, 1701.
- Trindade, J. R.; Visak, Z. P.; Blesic, M.; Marrucho, I. M.; Coutinho, J. A. P.; Canongia Lopes, J. N.; Rebelo, L. P. N. *J. Phys. Chem. B* **2007**, 111, 4737.
- Lopes, J. N. C.; Rebelo, L. P. N. *Chim. Oggi—Chem. Today* **2007**, 25, 37.
- Najdanovic-Visak, V.; Canongia Lopes, J. N.; Visak, Z. P.; Trindade, J.; Rebelo, L. P. N. *Int. J. Mol. Sci.* **2007**, 8, 736.
- Visak, Z. P.; Canongia Lopes, J. N.; Rebelo, L. P. N. *Monatsh. Chem.* **2007**, 138, 1153.
- Neves, C. M. S. S.; Ventura, S. P. M.; Freire, M. G.; Marrucho, I. M.; Coutinho, J. A. P. *J. Phys. Chem. B* **2009**, 113, 5194.
- Phillips, J. C.; Brauan, R.; Wang, W.; Gumbart, J.; Tajkhorshid, E.; Villa, E.; Chipot, C.; Skeel, R. D.; Kale, L.; Schulten, K. *J. Comput. Chem.* **2005**, 26, 1781.

- (31) Berendsen, H. J. C.; Postma, J. P. M.; van Gunsteren, W. F. *Intermolecular Forces*; D. Reidel Publishing Co.: Dordrecht, 1981.
- (32) Shi, W.; Maginn, E. J. *J. Chem. Theory Comput.* **2007**, *3*, 1451.
- (33) Cadena, C.; Maginn, E. J. *J. Phys. Chem. B* **2006**, *110*, 18026.
- (34) Canongia Lopes, J. N. A.; Pádua, A. A. H. *J. Phys. Chem. B* **2004**, *108*, 16893.
- (35) Jensen, K. P.; Jorgensen, W. L. *J. Chem. Theory Comput.* **2006**, *2*, 1499.
- (36) Cannon, W. R.; Pettitt, B. M.; McCammon, J. A. *J. Phys. Chem.* **1994**, *98*, 6225.
- (37) Bonhôte, P.; Dias, A. P.; Papageorgiou, N.; Kalyanasundaram, K.; Gratzel, M. *Inorg. Chem.* **1996**, *35*, 1168.
- (38) Tokuda, H.; Tsuzuki, S.; Susan, M. A. B. H.; Hayamizu, K.; Watanabe, M. *J. Phys. Chem. B* **2006**, *110*, 19593.
- (39) Voet, D.; Voet, J. G.; Pratt, C. W. *Fundamentals of Biochemistry*; John Wiley & Sons, Inc.: New York, 1999.
- (40) Freire, M. G.; Razzouk, A.; Mokbel, I.; Jose, J.; Marrucho, I. M.; Coutinho, J. A. P. *J. Chem. Eng. Data* **2005**, *50*, 237.
- (41) Kirkwood, J. G.; Buff, F. P. *J. Chem. Phys.* **1951**, *19*, 774.
- (42) General, I. J.; Ascuitto, E. K.; Madura, J. D. *J. Phys. Chem. B* **2008**, *112*, 15417.
- (43) Smith, P. E. *J. Phys. Chem. B* **2004**, *108*, 18716.
- (44) Aburi, M.; Smith, P. E. *J. Phys. Chem. B* **2004**, *108*, 7382.

JP9095634